Nigerian Research Journal of Chemical Sciences (ISSN: 2682-6054)
Volume 13, Issue 2, 2025

Exploring Metal-Ligand Interactions in $Ba(Ben)_4(CH_3COO)_2$ MOF: Synthesis, Spectroscopic Characterization, and Structural Analysis

Margaret D. Olawale
Department of Physical and Chemical Sciences,
Elizade University, Ilara-Mokin, Ondo State, Nigeria
Corresponding Author: olawalemargaret@gmail.com,
margaret.olawale@elizadeuniversity.edu.ng

Accepted: September 9, 2025. Published Online: September 16, 2025

ABSTRACT

This study reports the synthesis and characterization of a novel metal–organic framework, $Ba(Ben)_4(CH_3COO)_2$, prepared using benzoic acid as the ligand and barium acetate as the metal precursor. The reaction was carried out under reflux in ethanol and methanol, producing a stable white powdery precipitate with an 81% yield, highlighting the efficiency of the method. Characterization techniques included Infra-red (IR) and UV-Vis spectroscopy, elemental analysis, and powder X-ray diffraction (PXRD). IR spectra confirmed the coordination of benzoate ligands through carboxylate groups, with additional bands indicating acetate incorporation. UV-Vis spectra revealed π–π* and n–π* transitions, confirming the retention of the benzoic acid ligand. Elemental analysis supported the proposed molecular formula, while the absence of $M–OH_2$ bands indicated no water coordination. PXRD patterns displayed distinct differences from pure benzoic acid, confirming MOF formation, while preserving the structural integrity of the benzoate ligands and showing new peaks consistent with acetate incorporation. The coordination environment around barium is suggested to be octahedral, stabilized by benzoate and acetate ligands. These findings confirm the successful synthesis of $Ba(Ben)_4(CH_3COO)_2$ MOF and provide valuable insight into its structural properties and potential applications in materials science and catalysis.

Keywords: Metal-Organic Framework (MOF), benzoic acid ligand, spectroscopic characterization, ligand-metal interaction

INTRODUCTION

Metal-organic frameworks are a class of nanoporous coordination compounds formed through the reaction between inorganic metal ions and organic ligands [1,2]. These ligands can either be nitrogen-donor ligands, such as pyridine and phenanthroline, or oxygen-donor ligands, such as

carboxylates. The resulting structure is a chemically bonded coordination polymer with a three-dimensional geometry characterized by high porosity and large surface areas [1-4]. These unique properties make MOFs highly versatile, enabling their use in a wide range of applications, including gas sorption and storage [5], gas and vapor separation [2, 6], removal of industrial dyes and polycyclic aromatic hydrocarbons from wastewater [1,2,7], elimination of pharmaceutical contaminants from aqueous systems [8,9], heterogeneous catalysis for various chemical transformations [10,11], as well as advanced biomedical uses such as drug delivery and storage systems [12,13]. Oxygen-donor ligands are defined by the presence of oxygen atoms within their structure, which are available for binding with metal ions. Conversely, nitrogen-donor ligands contain nitrogen atoms in their structure, which can bond with the central metal ion [4, 10].

In recent years, metal-organic frameworks have garnered significant attention in materials science due to their remarkable porosity, which allows the accommodation of guest molecules within their hollow structures. The pattern and size of MOF pores are determined by the choice of organic ligands, while their flexible design is largely influenced by the synthetic routes employed. This flexibility enables the creation of a vast array of MOF structures, making them highly adaptable for various applications [11,12]. The exceptional porosity exhibited by metal-organic frameworks makes them highly suitable for various applications, including adsorption, separation, gas storage, catalysis, drug loading and delivery, vapor sensing, and other sensing technologies. A notable recent advancement in the field of MOFs is the synthesis of functional MOFs, leading to the development of functionalized MOF materials with exceptional properties. These materials demonstrate extraordinary loading capacities and high thermal stability, further enhancing their utility and making them even more advantageous for diverse applications [5, 13-14].

Research has shown that metal-organic frameworks exhibit excellent storage capacities, particularly for hydrogen in its gaseous state. The amount of gas adsorbed by a MOF depends on the pressure and temperature of the gas adsorbate. Generally, the rate of adsorption increases with rising pressure and decreases with increasing temperature [5, 13-14]. For example, MIL-53, synthesized by reacting aluminum salts with 1,4-benzene dicarboxylic acid, has a hydrogen adsorption capacity of 3.8 wt% [15]. Similarly, MOF-177 has demonstrated a hydrogen adsorption capacity of 7.5 wt% at 90 bar [6].

Metal-organic frameworks have been effectively applied for drug loading and delivery to targeted sites due to their tunable size, predetermined composition, and adjustable pore structure [13].

Research has demonstrated the synthesis of MIL-53(Fe) and MIL-53(Cr) MOFs, which were reported to achieve a maximum ibuprofen adsorption capacity of 17.4%. These MOFs also exhibited a controlled release time of up to 21 days in simulated body fluid [16, 17]. Additionally, Olawale et al. [8] synthesized a novel metal-organic framework, $[Ni(II)(Tpy)(Pydc)]\cdot 2H_2O$, which was used for the adsorption of caffeine from an aqueous drug solution. The results revealed that 1 gram of this MOF adsorbed 98.4 mg of caffeine. Olawale et al. [9] synthesized copper-glutamate metal-organic frameworks (MOFs) for the adsorption of aqueous ciprofloxacin. Their results revealed that 61.35 mg of ciprofloxacin was adsorbed per gram of copper-glutamate MOF.

Recently, MOFs have gained significant attention for their use in the adsorption of toxic and hazardous materials due to their exceptional properties. Tella et al. [7] synthesized $[Cd(INA)_2H_2O].ISB$ and employed it for the adsorption of methyl orange dye from an aqueous solution. The maximum adsorption capacity, calculated using the Langmuir model, was 166 mg/g [7]. Similarly, Lu et al. [18] evaluated the adsorption performance and kinetics of malachite green and methyl orange dyes using a Co-based MOF as the adsorbent. The Co-based MOF demonstrated high adsorption efficiencies of 99.0% and 90.5% for malachite green and methyl orange dyes, respectively, within 60 minutes of adsorption time. Olawale et al. [19] also utilized an activated $[Pb_4(Ben)_2(H_2O)]$ MOF to adsorb methyl red dye. The $[Pb_4(Ben)_2(H_2O)]$ exhibited excellent adsorption properties with high regeneration capacity.

The philosophy of this study lies in deepening the understanding of metal–ligand interactions within MOFs by synthesizing and characterizing a novel barium-based framework, $Ba(Ben)_4(CH_3COO)_2$. Whereas extensive research has been devoted to transition-metal MOFs such as those of Cu, Zn, and Zr, studies on alkaline-earth-metal-based MOFs remain comparatively limited. By employing benzoic acid and acetate ligands, this work explores how ligand coordination influences the stability, structural arrangement, and spectroscopic behavior of Ba-MOFs, thereby contributing to the broader development of MOFs as functional materials [19,20].

A notable knowledge gap addressed in this work is the scarcity of systematic investigations into the coordination chemistry of barium in MOFs, particularly with respect to structural integrity and ligand incorporation. The findings highlight $Ba(Ben)_4(CH_3COO)_2$ as a stable and well-defined framework with potential applications in heterogeneous catalysis, gas sorption and separation, and environmental remediation, especially in wastewater treatment and pollutant removal [21-23].

Therefore, this study provides valuable insights into the role of alkaline-earth metals in MOF design, opening avenues for their application in materials science and catalysis.

MATERIALS AND METHODS

The chemicals and reagents used in this research were of analytical grade and were procured from Sigma-Aldrich. Melting point determinations were conducted using a WRS-1B melting point apparatus. Elemental analyses were conducted using a Perkin-Elmer CHN Analyzer 2400 Series II. Infrared (IR) spectra were recorded with a SHIMADZU scientific model FTIR 8400S. Ultraviolet-visible (UV-Vis) spectrophotometric analyses were carried out using a PerkinElmer Lambda 25 UV Scanning Spectrophotometer, with spectra collected over the wavelength range of 200–800 nm for all samples.

Synthesis of $[Ba(Ben)_4(CH_3COO)_2]$ MOF

Benzoic acid (0.122 g, 1 mmol) was dissolved in 10 mL of ethanol, and barium acetate $[Ba(CH_3COO)_2]$ (0.13 g, 0.5 mmol) was dissolved in 10 mL of methanol. The two solutions were combined, and a few drops of triethylamine were added to facilitate the deprotonation of benzoic acid. The mixture was then refluxed at 200°C for 30 minutes with continuous stirring at 1000 revolutions per minute (rpm). During the reaction, a white precipitate formed, which was separated by filtration. The precipitate was washed thoroughly with a 1:1 mixture of methanol and ethanol to remove impurities and subsequently dried at room temperature in a desiccator.

RESULTS AND DISCUSSION

The reaction equation is provided in scheme 1:

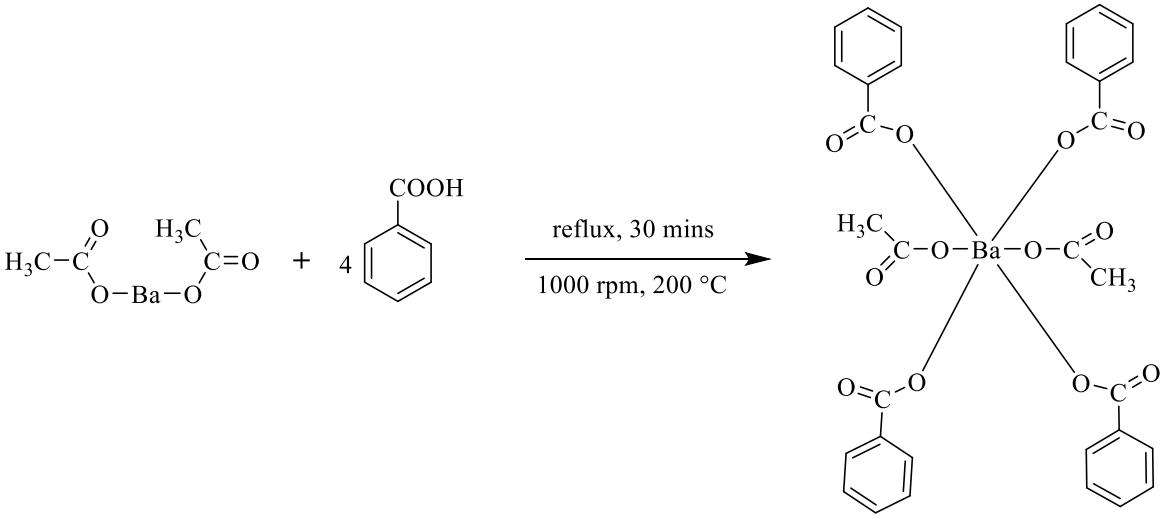

Scheme 1: The synthesis of $Ba(Ben)_4(CH_3COO)_2$ MOF

Yield: 81 %, M. wt. = 737.33, M. pt. = 176, Anal. Found (Calcd) % for [$C_{30}H_{26}O_8Ba$]: C, 54.43 (54.25); H, 3.81 (3.92); N, <0.10 (0.00), IR (KBr, cm^{-1}): 3062, 1697, 1521, 1307, 840, 518. UV-Vis (DMSO) nm: 211.

The synthesized metal-organic frameworks of benzoic acid were characterized using elemental analysis, infrared (IR) spectroscopy, UV-Vis spectroscopy, and powder X-ray crystallographic analysis. The analytical data, along with IR and UV-Vis spectroscopy results, are summarized in Table 1.

The elemental analysis of the $Ba(Ben)_4(CH_3COO)_2$ MOF aligned with its proposed formula unit, confirming the compound's composition. Spectroscopic studies and melting point analysis further supported the successful synthesis of the MOF. The color of the $Ba(Ben)_4(CH_3COO)_2$ MOF was similar to that of the ligand, indicating no significant change in visual properties (Table 1).

Table 1: Physical and Analytical Data of Benzoic acid and [$Ba(Ben)_4(CH_3COO)_2$]

Ligand/MOF	Appearance of ligand/ MOFs	Appearance of metal salt	Yield (%)	Molecular weight (g/mol)	Melting point (°C)	Elemental analysis % found (% calculated)		
						C	H	N
Benzoic acid	White powder	-	-	122.12	122.41	- (68.78)	- (4.91)	- (-)
[$Ba(Ben)_4(CH_3COO)_2$]	White powder	White	81	737.33	176	54.43 (54.25)	3.81 (3.92)	<0.10 (-)

The IR spectra of the MOF, showed notable differences compared to the ligand, which confirmed the bonding of the ligand to the metal ion (Table 2, Fig. 1).

Table 2: Selected FT-IR data (cm^{-1}) for Benzoic Acid and $Ba(Ben)_4(CH_3COO)_2$ MOF

FT-IR Absorption band	Benzoic acid	$Ba(Ben)_4(CH_3COO)_2$
ν(O-H) cm^{-1}	3068	-
ν_{as} (COO^- asymmetric stretch)	-	1550
ν_s (COO^- symmetric stretch)	-	1350
($\Delta\nu = \nu_{as} - \nu_s$)	-	200
ν(C-O) cm^{-1}	-	1235
ν(C=O) cm^{-1}	1791	1697
ν(C=C) cm^{-1}	1625	1521
ν(C=O) cm^{-1}	1650	-
ν(C-O) cm^{-1}	1328	-
ν(M-OH_2) cm^{-1}	-	-
ν(M-O) cm^{-1}	-	518
ν(C-H_3) cm^{-1}	-	1430

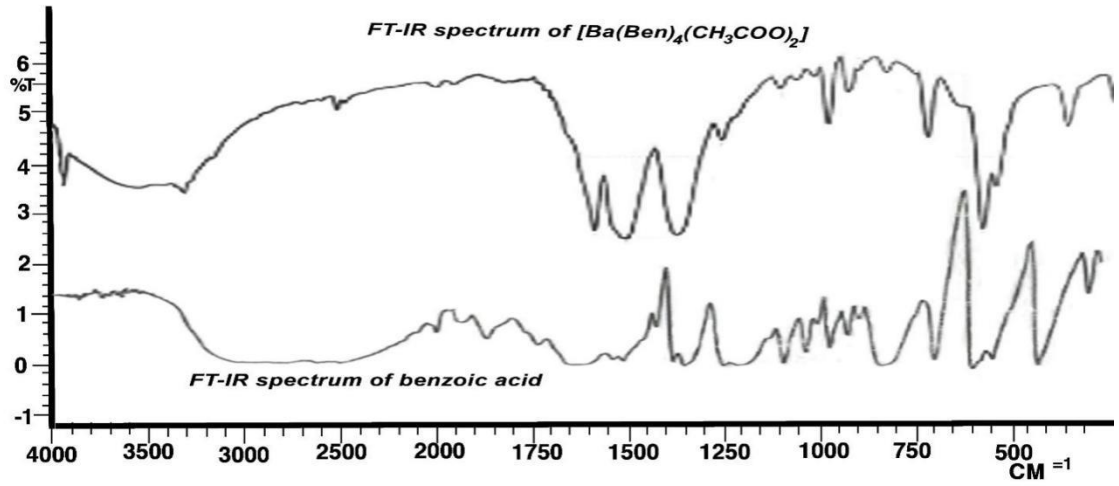

Fig. 1: Infrared spectra of benzoic acid and $Ba(Ben)_4(CH_3COO)_2$ MOF

The FT-IR spectrum of the $Ba(Ben)_4(CH_3COO)_2$ MOF revealed key features confirming coordination of the acetate ligand to the Ba^{2+} center. The free acetate vibrations observed in uncoordinated species at 1650 cm^{-1} (C=O) and 1328 cm^{-1} (C–O) were absent in the MOF, consistent with deprotonation and coordination through the carboxylate group. Instead, the spectrum displayed ν_as(COO^-) at 1550 cm^{-1} and ν_s(COO^-) at 1350 cm^{-1}, typical of coordinated carboxylates. The disappearance of the sharp C=O stretching band indicates that the resonance-stabilized carboxylate group is fully engaged in coordination rather than existing as a free carbonyl [24]. The separation between the asymmetric and symmetric carboxylate stretches ($\Delta\nu = 200$ cm^{-1}) provides further insight into the binding mode of acetate in the framework. According to established criteria, a large Δν value (>200 cm^{-1}) is diagnostic of monodentate coordination, whereas smaller values (100–150 cm^{-1} or <100 cm^{-1}) correspond to bridging or bidentate modes, respectively [25]. The observed Δν therefore confirms that acetate ligands coordinate to Ba^{2+} in a monodentate fashion within the MOF. These findings, together with complementary PXRD and UV–Vis analyses, provide strong evidence for the successful incorporation of acetate and the stabilization of the framework through Ba–O coordination.

The IR spectroscopy data further reveal that the C=C stretching vibration of the $Ba(Ben)_4(CH_3COO)_2$ MOF remains within the same range as that of the benzoic acid ligand. This observation confirms that the benzene ring in the ligand structure was preserved and did not undergo decomposition during the synthesis process. Additionally, the absence of the M-OH_2

absorption band in the IR spectrum of the $Ba(Ben)_4(CH_3COO)_2$ MOF indicates that water molecules are not coordinated to the metal center within the structure. This highlights the specificity of the coordination environment, where the benzoate ligand binds through its carboxylate group without interference from water molecules.

The appearance of the M–O absorption band at 518 cm^{-1} in the IR spectrum of the $Ba(Ben)_4(CH_3COO)_2$ MOF confirms the coordination of the metal ion to the benzoic acid ligand through the hydroxyl group of the carboxylic acid, following deprotonation [22]. This band is characteristic of the interaction between the metal center and the oxygen atoms, highlighting the successful incorporation of the ligand into the MOF structure.

The distinct C–H_3 absorption band at 1430 cm^{-1}, characteristic of the methyl group in acetic acid, further confirms the presence of acetate ions. This finding supports the conclusion that acetate is bonded to the metal ion, complementing the coordination environment established by the benzoate ligand. Together, these spectral features provide strong evidence for the successful formation of the $Ba(Ben)_4(CH_3COO)_2$ MOF with acetic acid playing a role in the coordination framework.

The UV-Visible spectra of benzoic acid and its complexes, as presented in Table 3 and Figure 2 and 3 demonstrate distinct differences between the free benzoic acid and the $Ba(Ben)_4(CH_3COO)_2$ MOF.

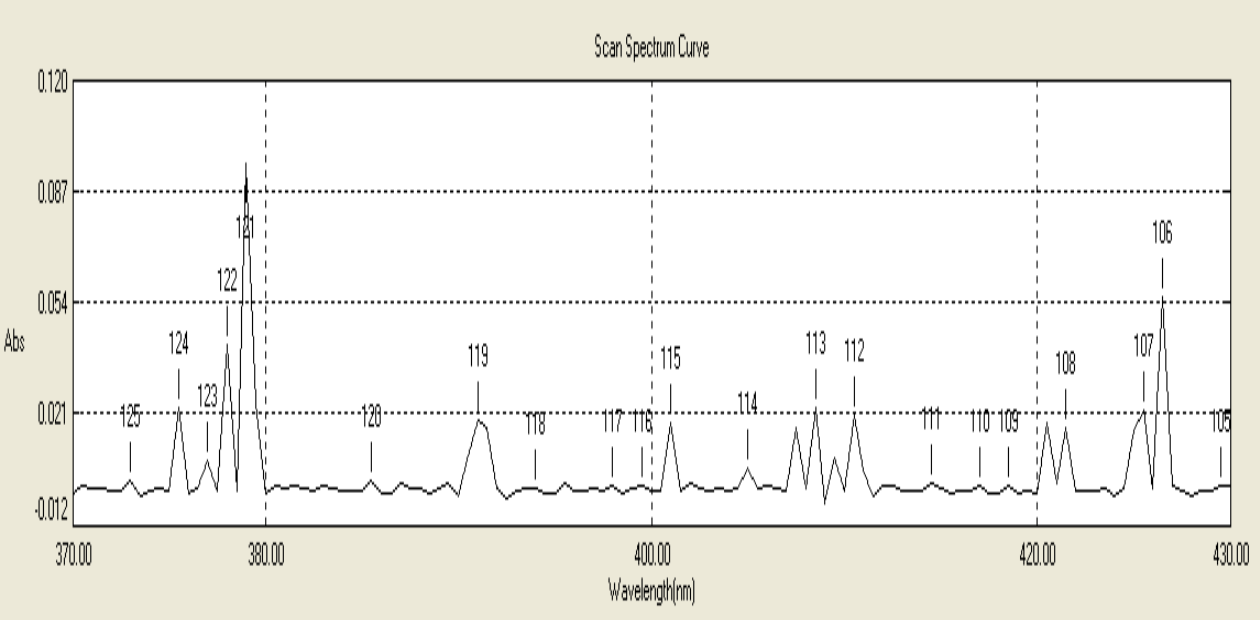

Fig. 2: visible spectrum of benzoic acid

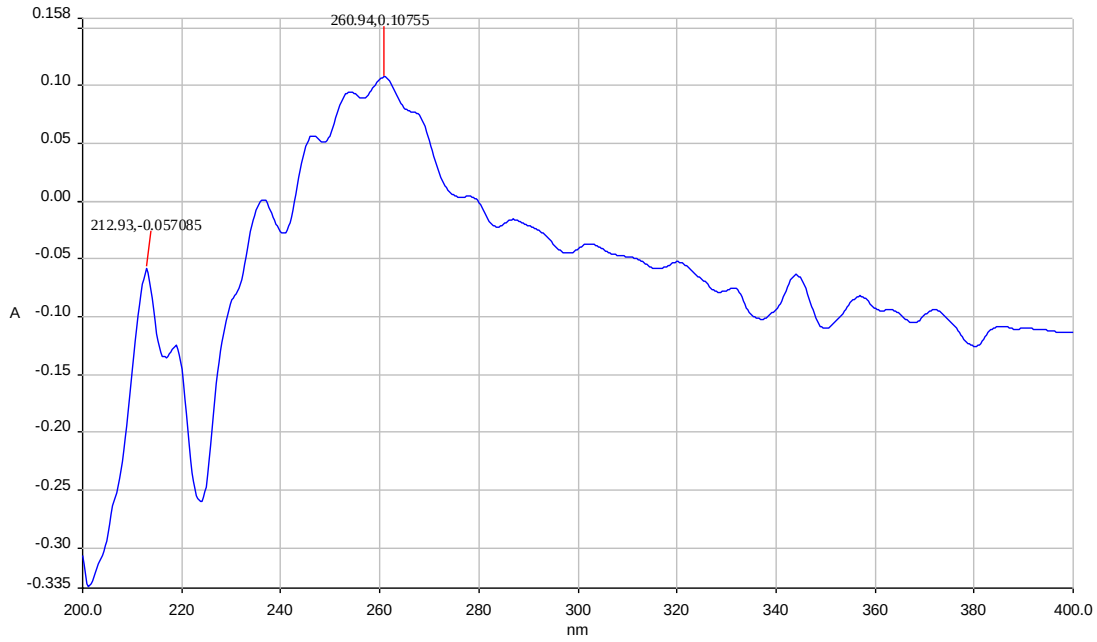

Fig. 3: Ultra-violet spectrum of $Ba(Ben)_4(CH_3COO)_2$ MOF

The MOF exhibits peaks that differ from those of free benzoic acid, indicating successful coordination of the benzoate ligand with the central metal ion. These spectral changes further confirm the formation of the metal-organic framework.

Table 3, Figures 2 and 3 present the UV-Vis spectra of benzoic acid and its complex, $Ba(Ben)_4(CH_3COO)_2$.

Table 3: UV-Visible Spectroscopy Data of Benzoic Acid and $Ba(Ben)_4(CH_3COO)_2$ MOF

Ligand/MOFs	Wavelength (nm)	Energy (cm-1)	Absorbance	Assignment
Benzoic acid	240	41666	0.004	$\pi - \pi^*$
	379	26315	0.096	$n - \pi^*$
$[Ba(Ben)_4.(CH_3COO)_2]$	211	47619	0.01	$\pi - \pi^*$
	No d-d transition			

The spectrum of benzoic acid displays characteristic bands at 240 nm and 397 nm, which correspond to the π-π* and n-π* transitions, respectively, associated with the C=C and C=O functional groups. These bands are also observed in the spectrum of the $Ba(Ben)_4(CH_3COO)_2$

MOF, confirming the presence of the benzoate ligand in the complex. Importantly, the $Ba(Ben)(CHCOO)_2$ MOF shows no additional bands beyond those associated with the π-π* and n-π* transitions, further confirming that the observed spectral features are solely due to the ligand's electronic transitions and not the presence of other chromophores.

Barium (II) ions (Ba^{2+}) do not exhibit any d–d transitions in the UV–Vis spectrum because of their electronic configuration. Unlike transition metals, which possess partially filled d-orbitals that can undergo electronic excitations under a ligand field, Ba^{2+} has a closed-shell configuration ([Xe]) with no d-electrons available for such transitions. Consequently, the observed UV–Vis absorptions in $Ba(Ben)_4(CH_3COO)_2$ MOF originate primarily from ligand-centered transitions such as π–π* and n–π* within the benzoate and acetate ligands, as well as possible ligand-to-metal charge transfer (LMCT) processes, rather than metal-centered d–d transitions. This distinction is consistent with the behavior of alkaline earth metal-based MOFs, where the metal nodes provide structural stability while the optical properties are largely governed by the organic linkers [26-25].

The powder X-ray diffraction (PXRD) patterns of the benzoic acid ligand were systematically compared with those of the $Ba(Ben)_4(CH_3COO)_2$ MOF to investigate structural differences and confirm successful synthesis. The PXRD spectra of the MOF exhibited significant dissimilarities in peak intensities and positions relative to the spectra of the ligand. These discrepancies indicate substantial structural modifications resulting from the incorporation of the benzoate ligand into the MOF framework, thereby confirming the successful formation of $Ba(Ben)_4(CH_3COO)_2$ MOF. Importantly, the presence of similar diffraction peaks in both spectra suggests that the benzoate ligand remains intact within the MOF structure, ruling out any decomposition or disintegration of the ligand during the synthesis process. This preservation of the ligand's integrity highlights its successful coordination within the MOF framework.

Additionally, new diffraction peaks were observed in the $Ba(Ben)_4(CH_3COO)_2$ MOF spectrum, which were absent in the benzoic acid ligand spectrum. These peaks are attributed to structural contributions from the acetate groups integrated into the MOF. The presence of these new peaks is a crucial indicator of the successful incorporation of both benzoate and acetate into the final MOF structure. The diffraction peaks of the benzoic acid ligand appeared over a range from 7.9° to beyond 40.0°, while the $Ba(Ben)_4(CH_3COO)_2$ MOF showed a distinct range of peaks from 11.1° to beyond 40.0°. Notably, specific new peaks at 11.5°, 11.7°, 14.7°, and 26.9° were identified in the MOF spectrum. These peaks may be attributed to unique structural features of the

$Ba(Ben)_4(CH_3COO)_2$ MOF, likely influenced by the coordination environment of the acetate and benzoate ligands within the MOF framework. The differences in PXRD patterns between the benzoic acid ligand and the synthesized MOF, along with the appearance of new characteristic peaks, strongly validate the successful synthesis of $Ba(Ben)_4(CH_3COO)_2$. The results also emphasize the role of the acetate groups in contributing to the structural characteristics of the MOF. These findings collectively demonstrate the formation of a robust and distinct crystalline framework incorporating both benzoate and acetate moieties.

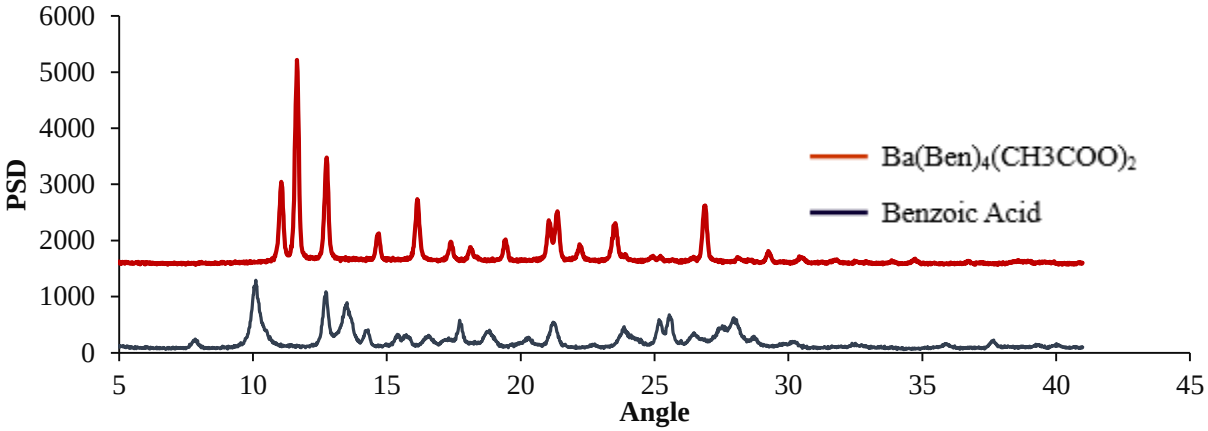

Fig. 3: Powder X-ray diffraction pattern of benzoic acid and $Ba(Ben)(CHCOO)_2$ MOF

This research study clearly demonstrates that the ligand forms bonds with the metal ion through the hydroxyl oxygen atoms of the carboxylate group in benzoic acid, as well as the hydroxyl oxygen of the acetate group originally bonded to the barium salt. These interactions confirm the dual coordination of the benzoate and acetate ligands to the central barium ion. Based on the observed coordination environment and spectral data, the geometry around the central barium ion is likely to be octahedral, with the ligands arranged symmetrically to satisfy the coordination requirements of the metal ion (Fig. 4).

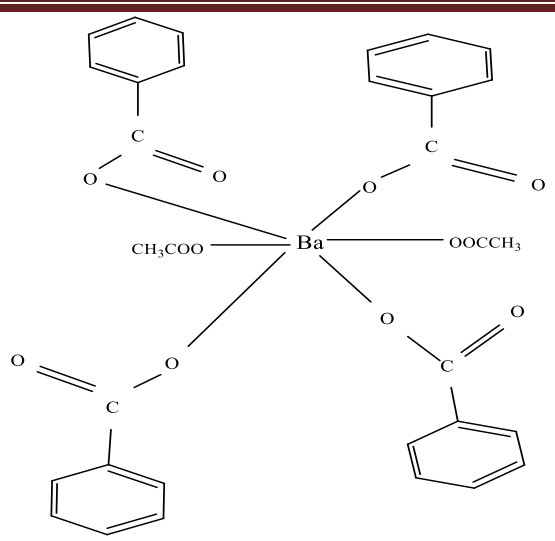

Fig. 4: Proposed Structure of Synthesized $Ba(Ben)_4.(CH_3COO)_2$

CONCLUSION

This study successfully synthesized and characterized the $Ba(Ben)_4(CH_3COO)_2$ metal-organic framework (MOF) using benzoic acid as the primary ligand and barium acetate as the metal precursor. The characterization results, including IR, UV-Vis spectroscopy, and elemental analysis, confirmed the successful coordination of the benzoate and acetate ligands to the barium ion. The IR spectral data revealed key shifts, such as the O-H band of the carboxylic group and the appearance of M-O and $C-H_3$ bands, providing strong evidence of ligand coordination and structural integrity.

The UV-Vis analysis highlighted the retention of the characteristic π-π^* and n-π^* transitions of the ligand within the MOF, confirming the preservation of the electronic properties of the benzoic acid ligand. The absence of additional peaks indicated the absence of extraneous chromophores, reinforcing the purity of the synthesized MOF.

The proposed octahedral geometry of the coordination environment around the barium ion is consistent with the bonding interactions observed between the carboxylate groups of the benzoate and acetate ligands and the metal center. The synthesis process also ensured the structural stability of the benzene ring in the ligand, as evidenced by the unaltered C=C stretching vibrations.

The PXRD analysis confirmed the successful synthesis of the $Ba(Ben)_4(CH_3COO)_2$ MOF, as evidenced by significant differences in diffraction peak positions and intensities compared to the benzoic acid ligand. The preservation of characteristic peaks from the ligand, along with the

emergence of new peaks unique to the MOF, verified the structural integrity of the benzoate ligand and the incorporation of acetate groups within the framework. These findings demonstrate the formation of a distinct crystalline structure, validating the coordination of both benzoate and acetate moieties in the $Ba(Ben)_4(CH_3COO)_2$ MOF.

The $Ba(Ben)_4(CH_3COO)_2$ MOF demonstrates a robust coordination framework and promising structural features, making it a valuable candidate for further applications in material science and catalysis.

REFERENCES

1. Tella, A. C., Olawale, M. D., Obaleye, J. A., Adimula, V. O., Alimi, L. O. & Ajibade, P. A. (2019) Removal of organic pollutant (pyrene) from aqueous solution using coordination polymer of $[Cu(Pic)_2(H_2O)_2]\cdot H_2O$ (CP-1) as adsorbent, *Applied Water Science*, 9, 1-12.
2. Zhou, H., Long, J. R. & Yaghi O. M. (2012) Introduction to Metal–Organic Frameworks, *Chem. Rev.*,112, 2, 673–674.
3. Olawale, M. D., Akintemi, E. O., Ojo, N. D., Isaac, A. Y., Su, H. & Obaleye, J. A. (2023) Synthesis, Characterization, Density Functional Theory, Monte Carlo, and Molecular Dynamics Simulations of $[Ni(II)(Tpy)_2]$ Metal Organic Framework and Congo Red Dye Application, *Journal of Computational Biophysics and Chemistry*, 22, (07), 845-862.
4. Oh, J.U., Sim, Y., Yang, G., Park, M., Kim, K. & Ryu, J. (2024) Surface functionalization of metal–organic framework nanoparticle for overcoming biological barrier in cancer therapy, *Inorg. Chem. Front.*, 11, 3119-3135.
5. Alhamami, M., Doan, H. & Cheng, C. A review on breathing behaviors of metal-organic-frameworks (MOFs) for gas adsorption, *Materials*, 7, 3198–3250.
6. Rowsell, J. L. & Yaghi, O. M. (2005) *Strategies for hydrogen storage in metal–organic frameworks.* Angew. Chemie Int. Ed. 2005, 44, 4670– 4679,
7. Tella, A. C., Olawale, M. D., Neuburger, M. & Obaleye, J. A. (2017) Synthesis and crystal structure of Cd-based metal-organic framework for removal of methyl-orange from aqueous solution. *Journal of Solid State Chemistry*, 225, 157-166.

8. Olawale, M. D., Obaleye, J. O. & Oladele, E. O. (2020) Solvothermal synthesis and characterization of novel [Ni (ii)(Tpy)(Pydc)]·$2H_2O$ metal–organic framework as an adsorbent for the uptake of caffeine drug from aqueous solution. *New Journal of Chemistry*, 44 (43), 18780-18791.
9. Olawale, M. D., Tella, A. C., Obaleye, J. A. & Olatunji J. S. (2020) Synthesis, characterization and crystal structure of a copper-glutamate metal organic framework (MOF) and its adsorptive removal of ciprofloxacin drug from aqueous solution. *New journal of chemistry*, 44 (10), 3961-3969.
10. Mueller, U., Schubert, M., Teich, F., Puetter, H. & Schierle-Arndt, K. P. (2006) Metal–organic frameworks—prospective industrial applications. *J Mater Chem*, 16, 626–636.
11. Zhang, X., Zhang, C., Yu, C. & Liu, C. (2024) Metal–organic frameworks for electrocatalytic hydrogen peroxide production. *Mater. Chem. Front*., 8, 1084-1100.
12. Tella, A. C., Obaleye, J. A., Olawale, M. D., Ngororabanga, J. M. V., Ogunlaja, A. S. & Bourne, S. A. (2019) Synthesis, crystal structure, and density functional theory study of a zinc (II) complex containing terpyridine and pyridine-2, 6-dicarboxylic acid ligands: Analysis of the interactions with amoxicillin, *Comptes Rendus. Chimie*, 22, (1), 3-12.
13. Tella, A. C., Olawale, M. D., Oyediran, A. O. & Alabi, A. B. (2020) Synthesis of Fe (III) Carboxylate Metal-Organic Framework Functionalized with Cetyltrimethylammonium Bromide and its Application for Loading Anti-hypertensive Drug. *J. Chem Soc. Nigeria* 45(1), 94 - 99.
14. Olawale, M. D., Ojo, N. D., Oyeneyin, O. E. & Tella A. C. (2025) Thermally Induced Solvent-Based Synthesis of Copper and Barium Metal–Organic Frameworks of Isonicotinic Acid: Characterization and Quantum Chemical Analysis of Electronic, Static, and Dynamic Optical Properties, *Chemistry Africa*, 1-18.
15. Férey, G., Latroche, M., Serre, C., Millange, F., Loiseau, T. & Percheron-Guégan, A. A. (2023) Hydrogen adsorption in the nanoporous metal-benzenedicarboxylate $M(OH)(O_2C–C_6H_4–CO_2)$ ($M = Al^{3+}$, Cr^{3+}), MIL-53, *Chem. Commun.* 24, 2976 – 2977.
16. Horcajada, P., Gref, R., Baati, T., Allan, P. K., Maurin, G., Couvreur, P., Ferey, G., Morris, R. E. & Serre, C. (2012) Metal–organic frameworks in biomedicine, *Chem. Rev*., 112, 1232– 1268.

17. Horcajada, P., Serre, C., Maurin, G., Ramsahye, N. A., Balas, F., Vallet-Regí, M., Sebban, M., Taulelle, F. & Férey, G. (2008) Flexible porous metal-organic frameworks for a controlled drug delivery. *J. Am. Chem. Soc*. 130, 6774– 6780.
18. Lu, H., Yang, Q., Huang, B., Qi, J., Wang, R., Zhou, Q., Chen, Q., Zhu, L., Jin, J. & Kong, Y. (2023) Removal performance and adsorption kinetics of dyes by a Co-based metal organic framework. *Microporous and Mesoporous Materials*, 360, 112665.
19. Olawale, M.D., Akintemi, E. O., Agbaffa, B. E. & Obaleye, J. A. (2022) Synthesis, characterization, adsorption study, quantum mechanics, monte carlo and molecular dynamics of lead based polymeric compound towards mopping of aqueous methyl red dye. *Result in Chemistry*, 4, 1-18.
20. Furukawa, H., Cordova, K. E., O'Keeffe, M., & Yaghi, O. M. (2013). The chemistry and applications of metal-organic frameworks. *Science*, 341(6149), 1230444.
21. Li, J. R., Kuppler, R. J., & Zhou, H. C. (2009). Selective gas adsorption and separation in metal–organic frameworks. *Chem. Soc. Rev.*, 38(5), 1477–1504.
22. Olawale, M. D., Ojo, N. D., Oyeneyin, O. E., Adimula, V. O. & Siyanbola T. O. (2025) Synthesis, Electronic, Dynamic Optical and Adsorption (Monte Carlo and Molecular Dynamics) Properties of Cadmium Picolinate Coordination Polymer-2 (Cp-2). *Journal of Computational Biophysics and Chemistry*. 1-15.
23. Olawale, M.D., Obaleye, J.A. & Oladele, E.O. (2020) Itaconic acid based coordination polymer: mechanochemical synthesis, characterization and vapochromic study, *Nigerian Research Journal of Chemical Sciences*, 8 (1), 280-290.
24. Nakamoto, K. Infrared and Raman Spectra of Inorganic and Coordination Compounds, 6th ed.; Wiley: New York, 2009.
25. Deacon, G. B. & Phillips, R. (1980) J. Relationships between the carbon–oxygen stretching frequencies of carboxylato complexes and the type of carboxylate coordination. *Coord. Chem. Rev.*, 33, 227–250.
26. Cotton, F. A., Wilkinson, G., Murillo, C. A., Bochmann, M. Advanced Inorganic Chemistry, 6th Ed., Wiley, 1999.
27. Atkins, P., Overton, T., Rourke, J., Weller, M., Armstrong, F., Shriver & Atkins' Inorganic Chemistry, 5th Ed., Oxford University Press, 2010.
28. Zhou, H. C., Long, J. R. & Yaghi, O. M. (2012) Metal–organic frameworks (MOFs): structures and applications. *Chem. Rev*., 112, 673–674.